Supplementary Information for

Tuning electrolyte enables microsized Sn as advanced anode for Li-ion batteries

Nan Zhang [a], Chuangchao Sun [a], Yiqiang Huang [a], Chunnan Zhu [a], Zunchun Wu [a], Ling Lv [a], Xiuquan Zhou [b], Xuancheng Wang [a], Xuezhang Xiao [a], Xiulin Fan*[a], and Lixin Chen*[a]

[a] *State Key Laboratory of Silicon Materials, School of Materials Science and Engineering, Zhejiang University, Hangzhou 310027, China. E-mail: xlfan@zju.edu.cn; lxchen@zju.edu.cn*

[b] *Department of Chemistry and Biochemistry, University of Maryland, College Park, MD 20742, USA*

1. Supplementary Note

1.1 Supplementary Note 1

Discussion of the separators using in half cells and full cells

The purpose of using two seperators (PP and GF) was not to store more electrolyte, but to prevent the micro short circuit caused by the growth of lithium dendrite. Though the specific principles have not yet been thoroughly studied, we guess that the SEI formed on the lithium foil (the counter electrode in half cells) is too thin to prevent the growth of lithium dendrite. As a result, in the delithiation process, lithium dendrite generated on the surface of lithium foil will pierce a single PP separator and lead to the micro short circuit (Figure S1a). Once the micro short circuit occurred, much more parasite reaction will happen, leading to reduced cycle lifespan and untrustworthy columbic efficiency (far more than 100%). We also tested the cycle stability of half cells with a single PP separator and limited electrolyte (50 μL). Although severe parasite reaction did occur, such cells still exhibited acceptable cycling stability (Figure S1b), indicating excessive electrolyte is not necessary. In fact, when we assembled half cells with two separators, electrolyte of ~150 μL was added to each CR2025 coin cells (it is inevitable to use more electrolyte to ensure the wet of separators). Moreover, 2-MeTHF-based electrolytes show excellent wet ability when PP separators is applied and there is no lithium metal in full cells, so we use a single PP separator and limited electrolyte to assemble full cells, showing no bad impact on the energy density of full cells.

1.2. Supplementary Note 2

Discussion of chemical stability of LiPF6 ether electrolytes

Although ether-based electrolytes showed promising prospects for alloy anodes, not all ethers are adaptable with the most common salt, $LiPF_6$. Only several ethers with a specific structure exhibit good compatibility with $LiPF_6$. We studied the physical state changes of various commonly used ethers solvents containing 1.0 M $LiPF_6$ along with time, including THF, 2-MeTHF, THF/2-MeTHF (THF: 2-MeTHF = 1:1, vol), dimethoxyethane (DME), 1,3-dioxolane (DOL). At the very beginning of adding 1.0 M $LiPF_6$ to the mentioned 5 ether solvents and baseline EC/DMC solvent, colorless (or slightly yellow) and transparent solutions were acquired for all the above solvents. After only 5 minutes, a violent reaction accompanied heat generation was observed in DOL solvent, and the overall solution transformed to gelatinous soon. The reaction of $LiPF_6$ with $LiPF_6$ and DME occurred soon after and lasted for several days. Eventually, the whole solution of THF electrolyte and ~1/3 of DME electrolyte converted to gelatinous. There is no obvious state change in 2-MeTHF, THF/2-MeTHF, and EC/DMC solutions after 1 month.

1.3. Supplementary Note 3

Discussion of phase transition of SnMP during the charge/discharge

During the charge/discharge process, SnMPs have gone through multiple steps and the full lithiated phase was $Li_{22}Sn_5$, which has been discussed in the main body. However, more detailed phase transformation and the formation of Li_ySn (y≈2.5) were not mentioned. Rhodes et al.[1] believed there were four phases, including tin, Li_2Sn_5, LiSn, and $Li_{22}Sn_5$, during the lithiation process of pristine Sn via an in-situ XRD of thin film tin electrodes for lithium-ion batteries. However, the results were not well-matched with the plateaus and slopes we obtained in the charge/discharge curves. The endpoint of the longest plateau (approximately alloying 2.5 Li atoms for each Sn atom) means the full conversion of a new phase from LiSn. Yet the XRD information was less clear due to the difficulty of clearly discriminating between several possible Li_ySn ($y \approx 2.5$) phases, namely Li_5Sn_2, Li_7Sn_3, and $Li_{13}Sn_5$, which was consistent with the work of Antitomaso et al[2]. We finally use Li_ySn ($y \approx 2.5$) to represent the phase and the chemical equations can thus be written as follows:

$$Sn + 0.4Li \rightarrow 0.2Li_2Sn_5$$
$$0.2Li_2Sn_5 + 0.6Li \rightarrow LiSn$$
$$LiSn + (y - 1)Li \rightarrow Li_ySn\ (y \approx 2.5)$$
$$Li_ySn + (4.4\text{-}y)Li \rightarrow 0.2Li_{22}Sn_5$$

2. Supporting Figures

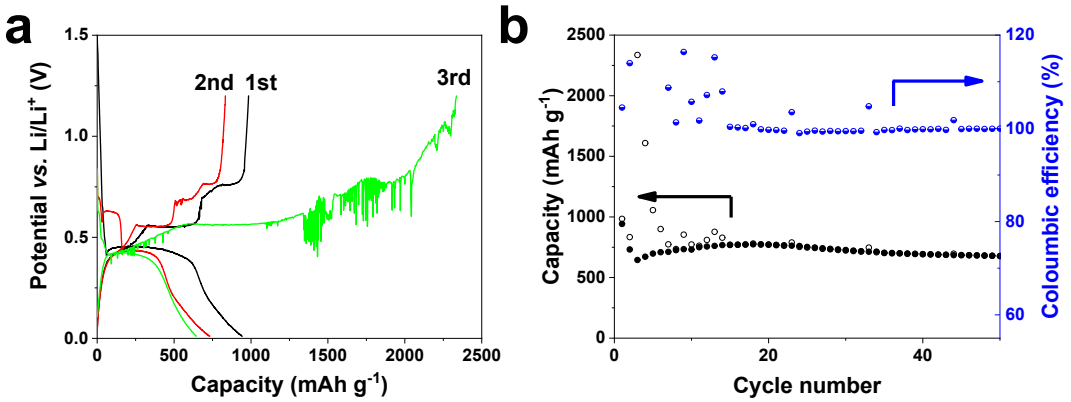

Fig. S1 a) The voltage profiles of 1st-3rd cycle and b) cycle performance of the half cell with a single PP separator and 50 μL electrolyte.

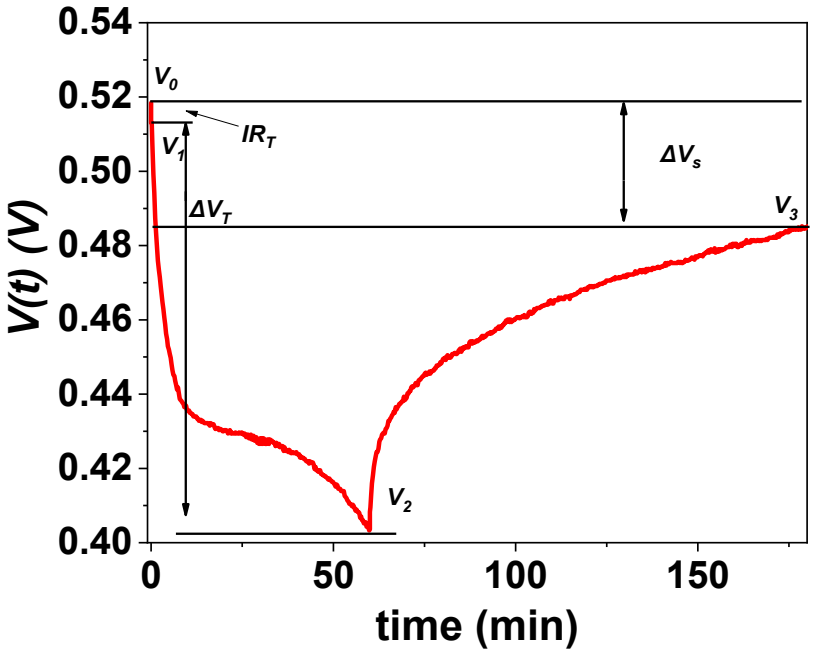

Fig. S2 A typical magnified voltage-time profile of one discharge pulse derived from GITT.

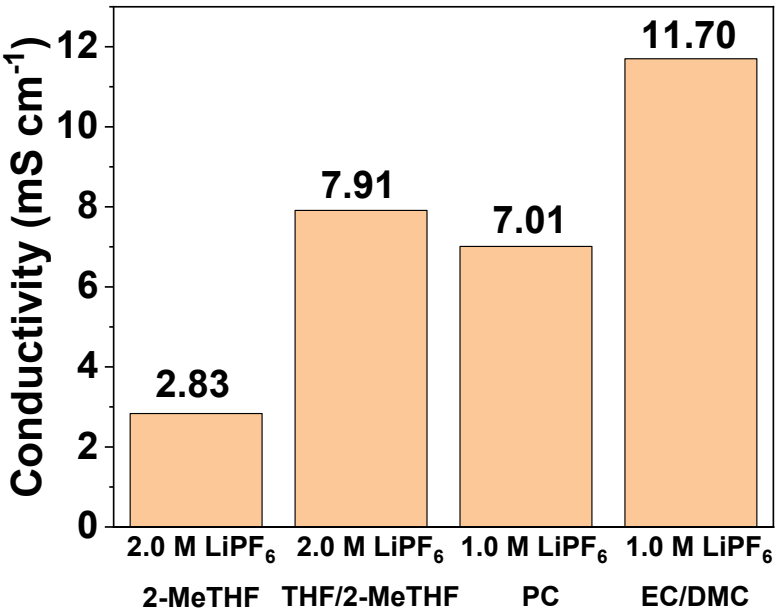

Fig. S3 Ionic conductivity of various electrolytes: 1# 2.0 M $LiPF_6$ 2-MeTHF, 2# 2.0 M $LiPF_6$ THF/2-MeTHF, 3# 1.0 M $LiPF_6$ PC, 4# 1.0 M $LiPF_6$ EC/DMC

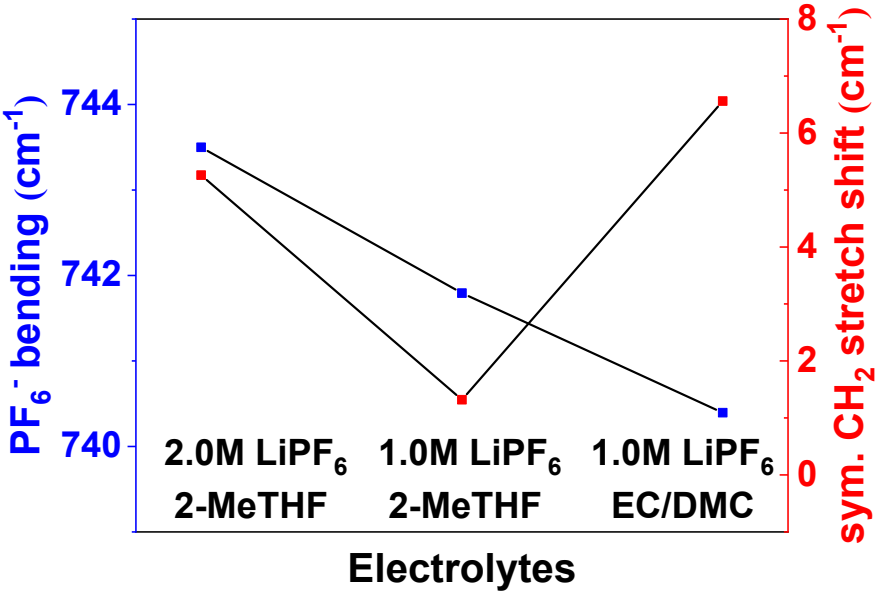

Fig. S4 The peak shift trend of PF_6^- and CH_2 stretch.

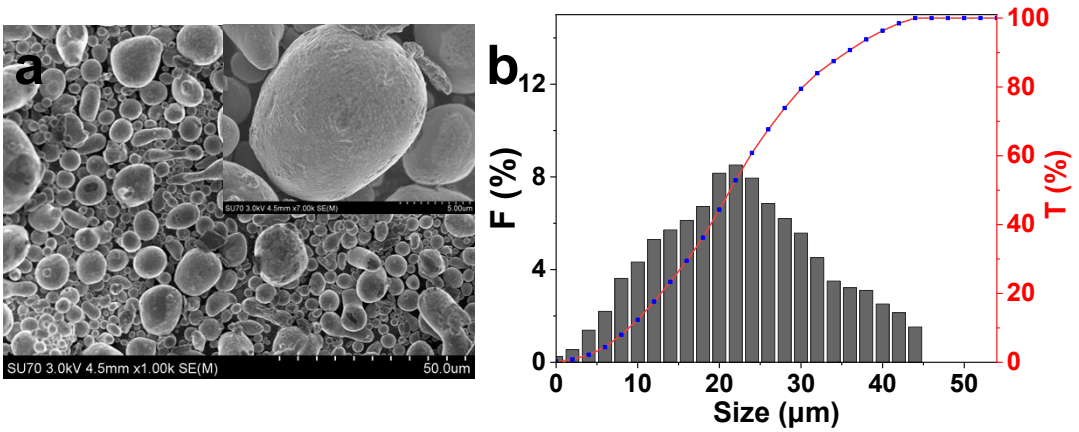

Fig. S5 a) SEM image of SnMPs, b) diameter distribution of SnMPs.

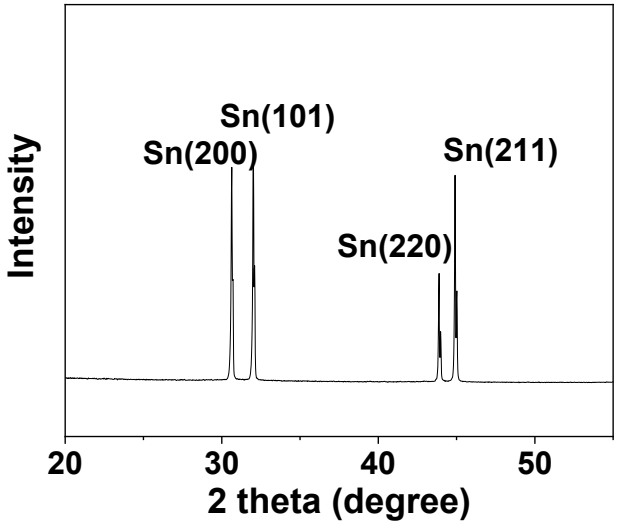

Fig. S6 XRD pattern of SnMPs

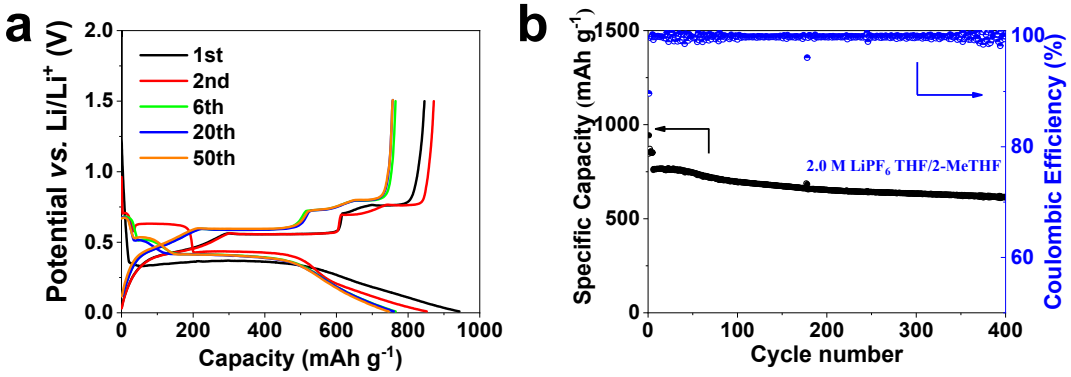

Fig. S7 a) Typical charge/discharge profiles and b) Cycling stability and CE of SnMP electrode cycled in 2.0 M $LiPF_6$ THF/2-MeTHF. The rates were C/5 at the initial 5 cycles and 2C at the subsequent cycles.

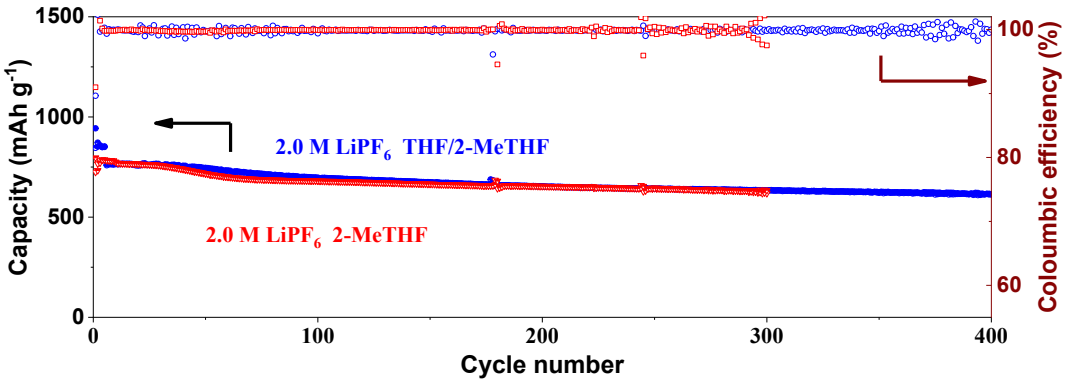

Fig. S8 Cycling stability of SnMPs in 2.0 M $LiPF_6$ THF/2-MeTHF (blue) and 2.0 M $LiPF_6$ 2-MeTHF (red).

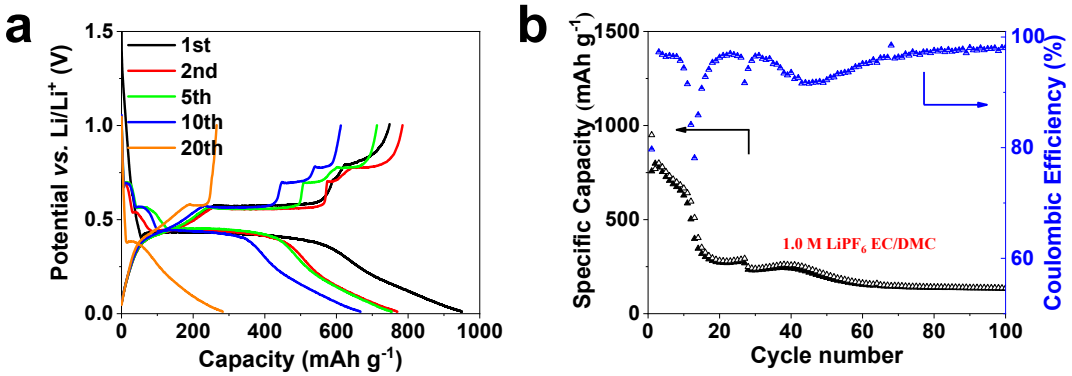

Fig. S9 a) Typical charge/discharge profiles and b) Cycling stability and CE of SnMP electrode cycled in 1.0 M $LiPF_6$ EC/DMC. The rate was C/5.

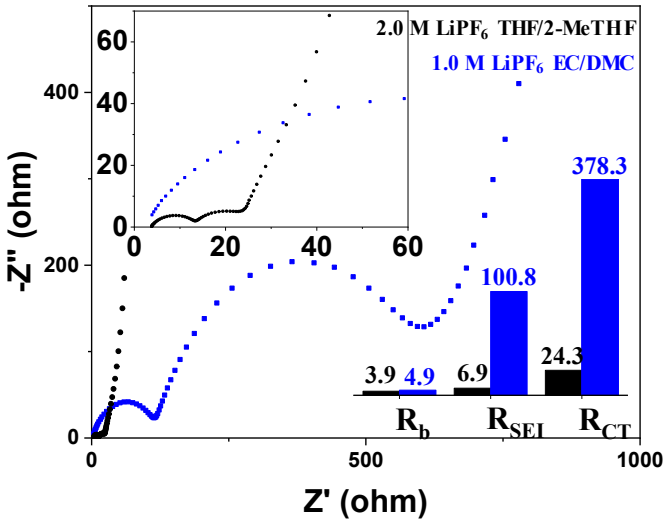

Fig. S10 EIS in Nyquist plots of SnMPs in 2.0 M $LiPF_6$ THF/2-MeTHF electrolyte (black), 1.0 M $LiPF_6$ EC/DMC electrolyte (blue).

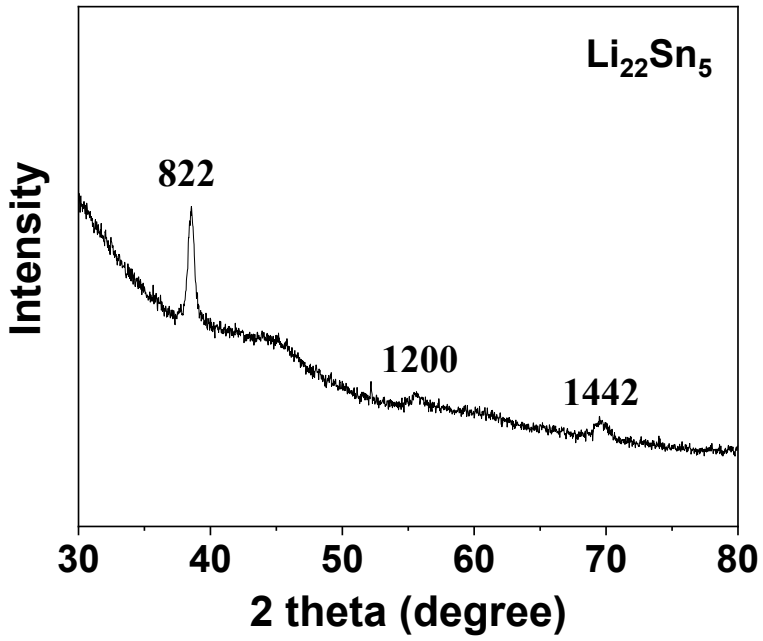

Fig. S11 XRD pattern of the final lithiated phase $Li_{22}Sn_5$.

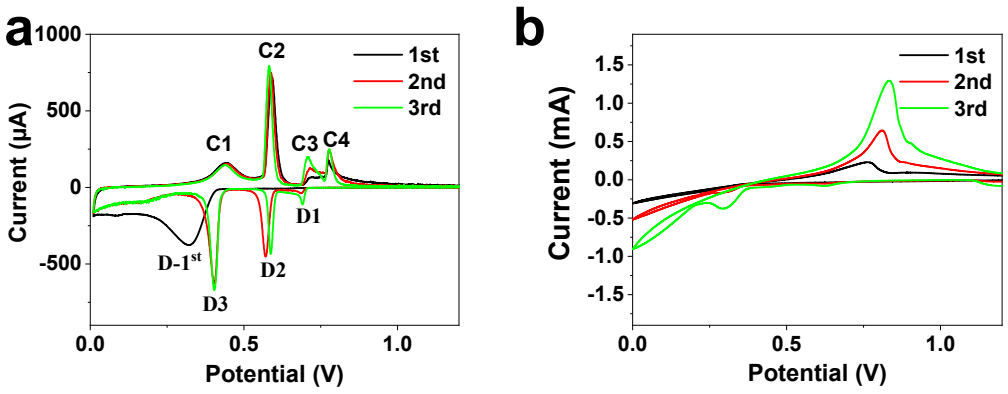

Fig. S12 a) CV curves of SnMPs cycled in 2.0 M $LiPF_6$ THF/2-MeTHF electrolyte b) CV curves of SnMPs cycled in 1.0 M $LiPF_6$ EC/DMC electrolyte.

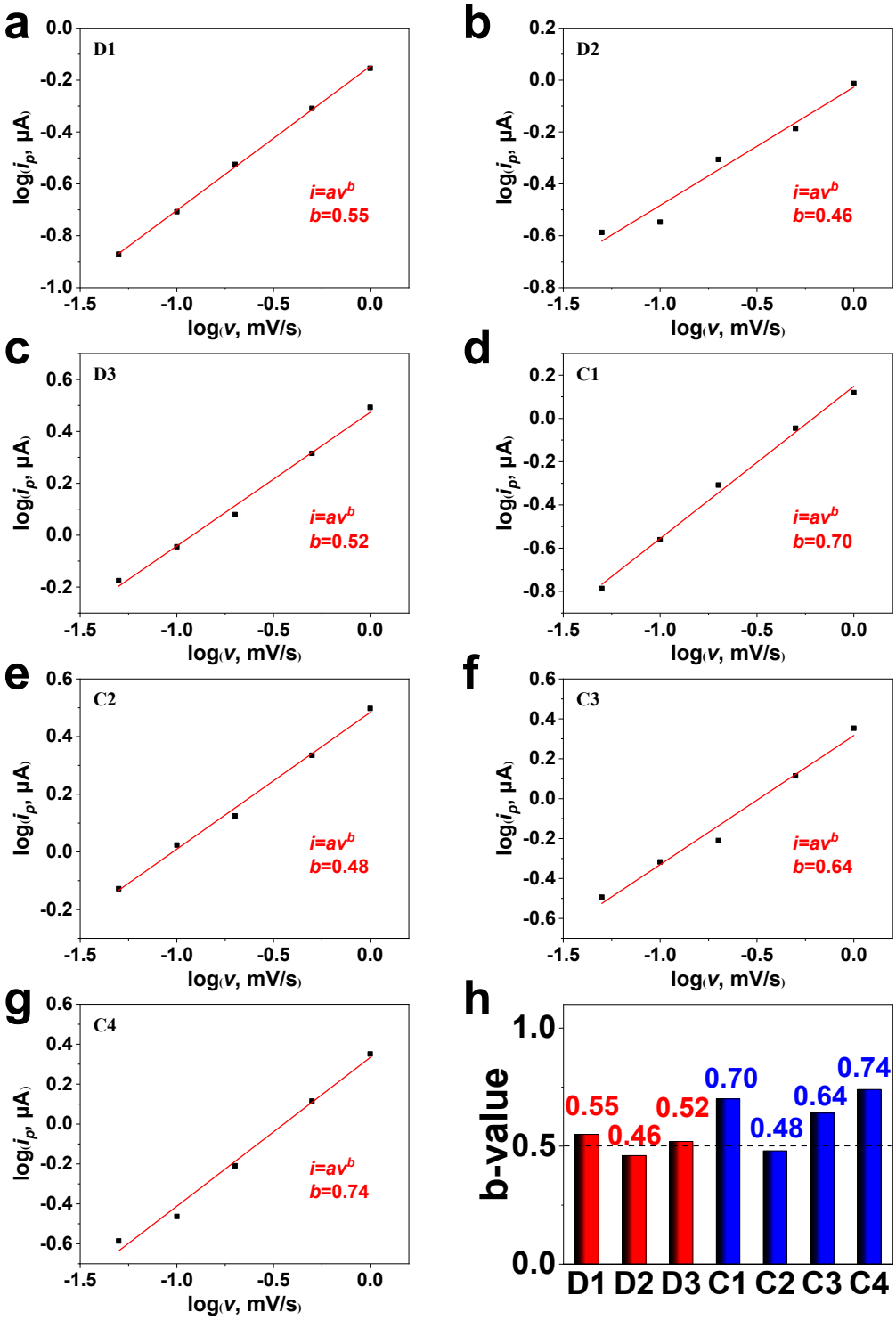

Fig. S13 a)-g) Log i (peak current) vs log υ (scan rate) plots at charging/discharging from the CV curves of SnMPs. h) b-values of different peaks.

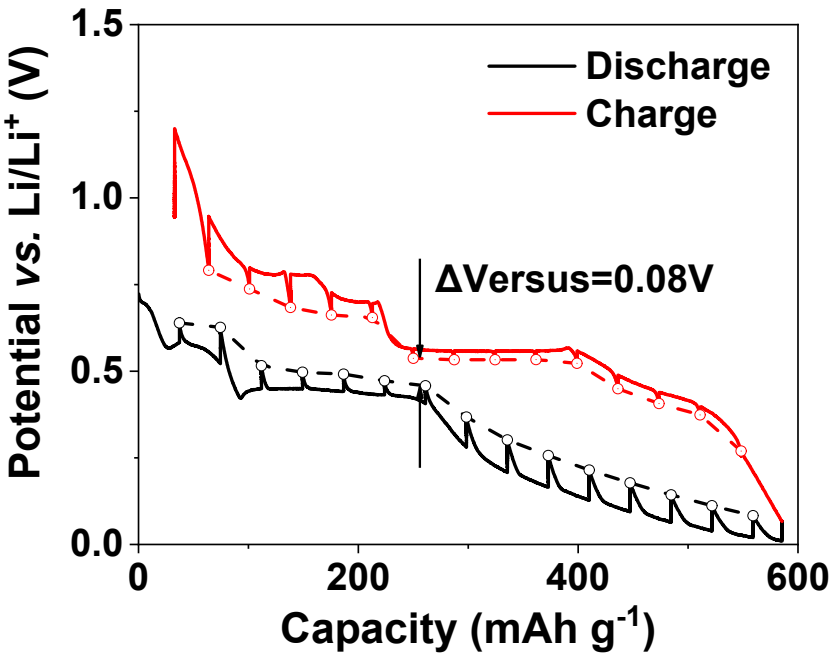

Fig. S14 GITT profiles of SnMPs in 1.0 M $LiPF_6$ EC/DMC

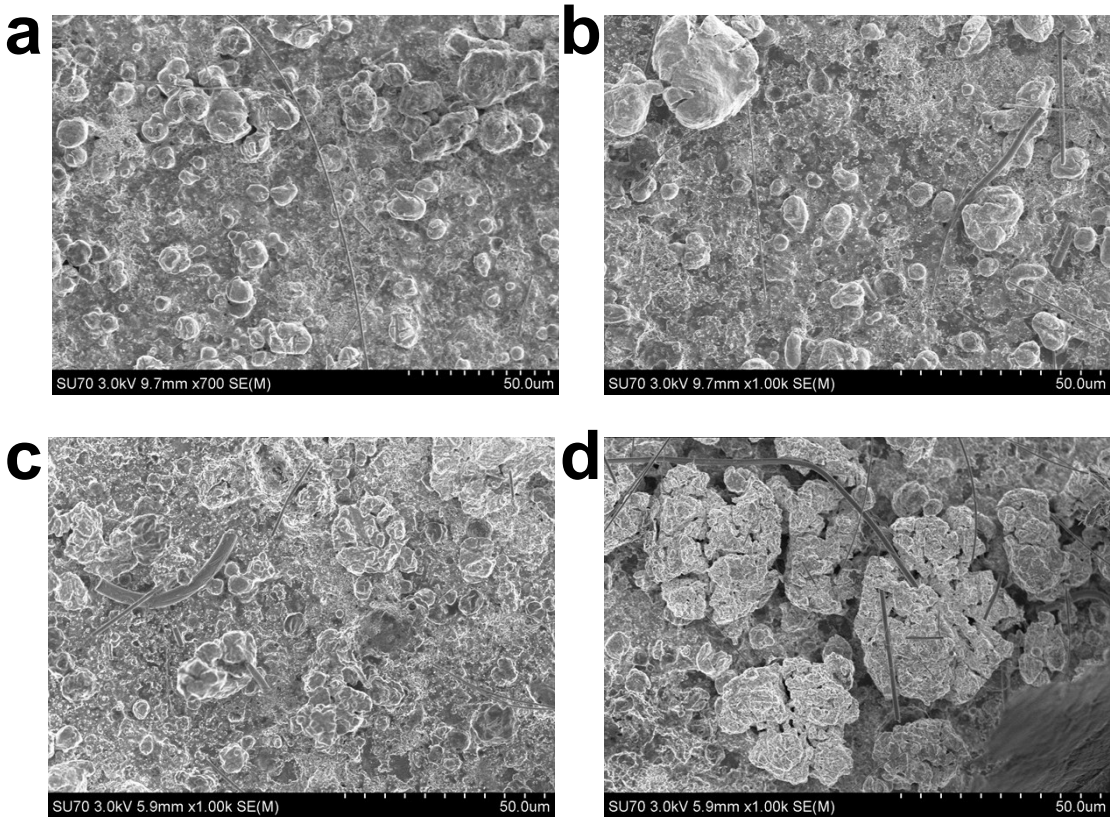

Fig. S15 SEM images at lower magnification of SnMPs cycled in 2-MeTHF-based electrolyte after a) 1 cycle, b) 5 cycles; c), d) SnMPs cycled in 1.0 M EC/DMC electrolyte after 1 cycle.

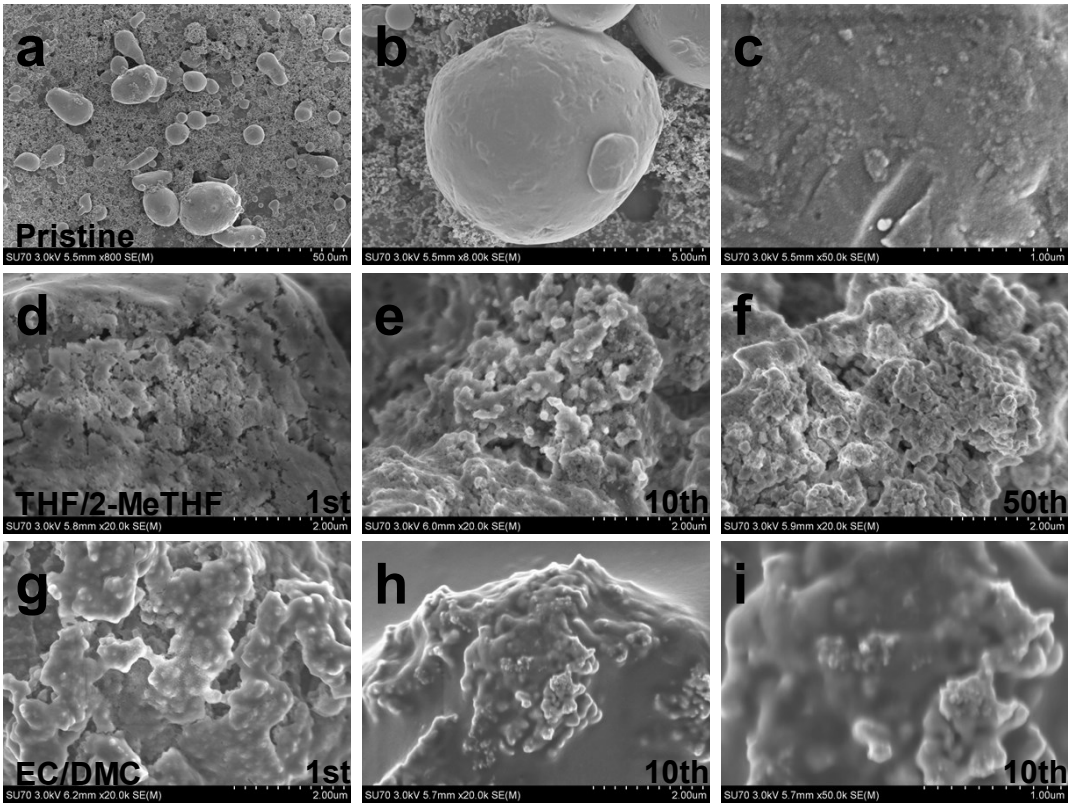

Fig. S16 SEM images of a), b) c) pristine SnMPs. d), e), f) SnMPs cycled in 2.0 M $LiPF_6$ THF/2-MeTHF electrolyte after 1, 10, 50cycles. g), h), i) SnMPs cycled in 1.0 M $LiPF_6$ EC/DMC electrolyte after 1, 10 cycles.

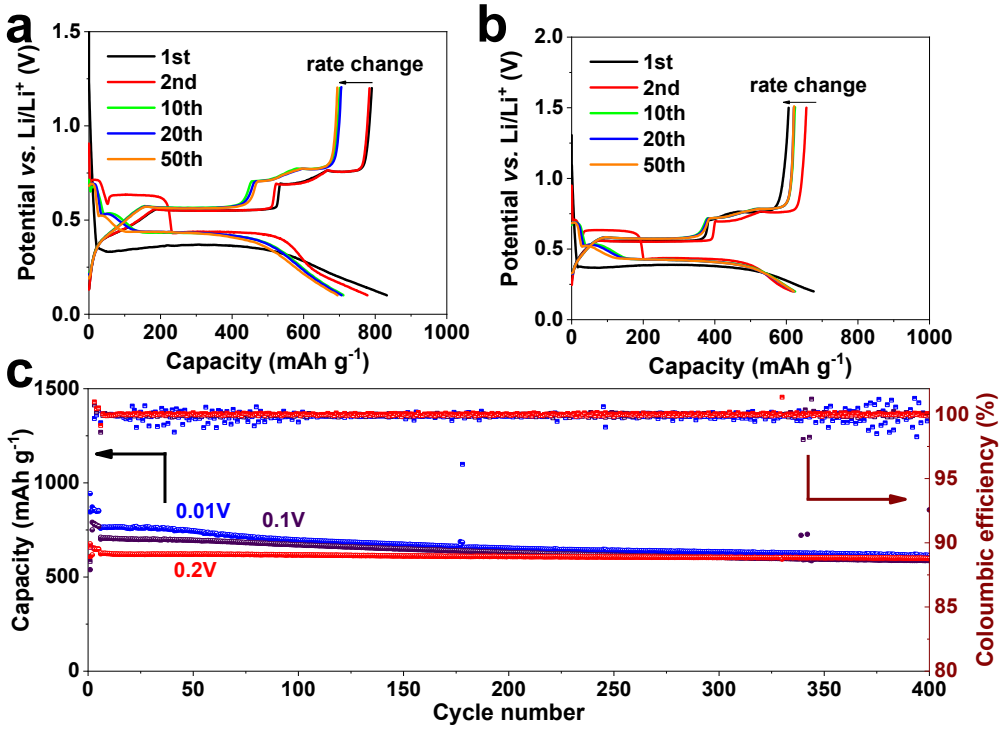

Fig. S17 Voltage profiles of SnMPs cycled in 2.0 M $LiPF_6$ THF/2-MeTHF electrolyte with a) 0.1V, b) 0.2V cut-off voltage. c) Cycling performance of SnMPs cycled with various cut-off voltages.

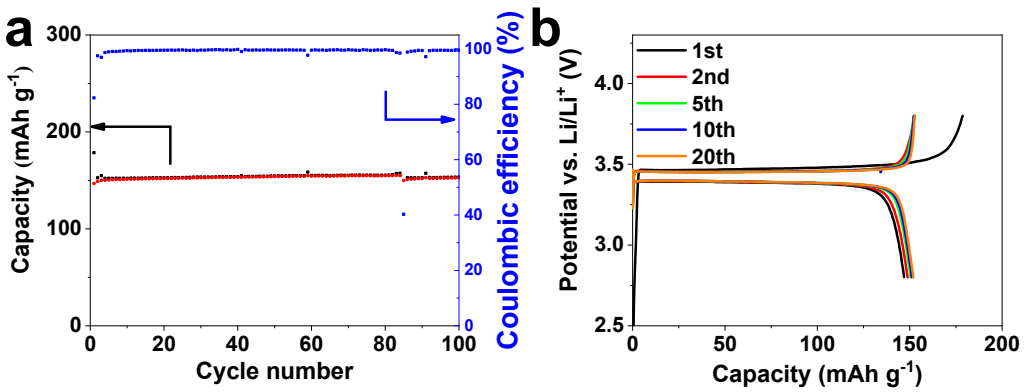

Fig. S18 a) Voltage profiles and b) cycling performance of LFP cathode cycled in 2.0 M $LiPF_6$ THF/2-MeTHF electrolyte.

Notes and references

[1] K. J. Rhodes, R. Meisner, M. Kirkham, N. Dudney, C. Daniel, *J. Electrochem. Soc.*, 2012, **159**, A294-A299.
[2] P. Antitomaso, B. Fraisse, L. Stievano, S. Biscaglia, D. Ayme-Perrot, P. Girard, M. T. Sougrati, L. Monconduit, *J Mater. Chem. A*, 2017, **5**, 6546-6555.